Genuine phase diffusion of a Bose-Einstein condensate in the microcanonical ensemble: A classical field study

A. Sinatra and Y. Castin
Laboratoire Kastler Brossel, Ecole Normale Supérieure, Université Pierre et Marie Curie and Centre National de la Recherche Scientifique, 24 Rue Lhomond, 75231 Paris Cedex 05, France
(Received 10 August 2008; revised manuscript received 9 October 2008; published 10 November 2008)

Within the classical field model, we find that the phase of a uniform Bose-Einstein condensate at nonzero temperature undergoes a true diffusive motion in the microcanonical ensemble, the variance of the condensate phase change between time zero and time t growing linearly in t. The phase diffusion coefficient obeys a simple scaling law in the double thermodynamic and Bogoliubov limit. We construct an approximate calculation of the diffusion coefficient, in fair agreement with the numerical results over the considered temperature range, and we extend this approximate calculation to the quantum field.

DOI: 10.1103/PhysRevA.78.053615 PACS number(s): 03.75.Kk

I. INTRODUCTION

Phase coherence is one of the most prominent properties of Bose-Einstein condensates, relevant for applications of condensates in metrology and quantum information [1]. The issue of condensate phase dynamics and phase spreading at zero temperature due to interactions has been extensively studied in theory [2] and experiments [3–5]. There is a renewed interest in this issue of temporal phase coherence due to the recent studies in low-dimensional quasicondensates, both experimentally [6–8] and theoretically [9]. The present work addresses the problem of the determination of fundamental limits of phase coherence in a true three-dimensional Bose-Einstein condensate at nonzero temperature.

The effect of a nonzero temperature on phase coherence in a Josephson junction realized by a condensate trapped in a double well potential has been studied in [10,11]. The situation is different when the two condensates are separated. In this case there is no restoring force for the relative phase which then evolves independently in the two Bose-Einstein condensates (BECs) [12]. The effect of thermal fluctuations in this case, joint to the effect of the interactions, is to provide a spreading in time of the relative phase.

In a previous work [13], we considered a condensate prepared in an equilibrium state in the canonical ensemble. In that case we could show using ergodicity that the phase change of the condensate during a time t has a variance which grows proportionally to t^2. In other words, the condensate phase spreading in the canonical ensemble is ballistic [14] and not diffusive [15–18]. As we could calculate in [13] using an ergodic theory, the coefficient of this superdiffusive thermal spreading is proportional to the variance of the energy in the considered equilibrium state. If we now suppress the fluctuations of energy in the initial state, by moving from the canonical ensemble to the microcanonical ensemble, the ballistic thermal spreading disappears and one may expect that the condensate phase undergoes a genuine diffusion in time. In the present work we show that this is indeed the case and we study this genuine phase diffusion numerically within the classical field model [19–22] described in Sec. II. The numerical results are presented in Sec. III, and their analysis shows the existence of simple scaling laws and of a universal curve giving the phase diffusion coefficient in the double thermodynamical limit (atom number $N\to\infty$, volume $V\to\infty$, density $\rho=$const) and Bogoliubov limit ($N\to\infty$, coupling constant $g\to 0$, $Ng=$const). In Sec. IV we derive an aproximate formula for the diffusion coefficient that we compare to the numerical results and that we also extend to the quantum field. We conclude in Sec. V.

II. CLASSICAL FIELD MODEL AND NUMERICAL PROCEDURE

We consider a lattice model for a classical field $\psi(\mathbf{r})$ in three dimensions. The lattice spacings are l_1, l_2, l_3 along the three directions of space and $dV=l_1l_2l_3$ is the volume of the unit cell in the lattice. We enclose the atomic field in a spatial box of sizes L_1, L_2, L_3 and volume $V=L_1L_2L_3$, with periodic boundary conditions. To guarantee efficient ergodicity in the system we choose noncommensurable square lengths in the ratio $L_1^2:L_2^2:L_3^2=\sqrt{2}:(1+\sqrt{5})/2:\sqrt{3}$. The lattice spacings squared l_1^2, l_2^2, l_3^2 are in the same ratio.

The field ψ may be expanded over the plane waves

$$\psi(\mathbf{r})=\sum_{\mathbf{k}} a_{\mathbf{k}}\frac{e^{i\mathbf{k}\cdot\mathbf{r}}}{\sqrt{V}}, \tag{1}$$

where $\mathbf{k}$ is restricted to the first Brillouin zone, $k_\alpha \in [-\pi/l_\alpha,\pi/l_\alpha[$ and α labels the directions of space.

We assume that, in the real physical system, the total number of atoms is fixed, equal to N. In the classical field model, this fixes the norm squared of the field:

$$dV\sum_{\mathbf{r}}|\psi(\mathbf{r})|^2=N \tag{2}$$

or equivalently the mean density of the system

$$\rho=\frac{N}{V} \tag{3}$$

for each realization of the field. The evolution of the field is governed by the Hamiltonian [23]

$$H = \sum_{\mathbf{k}} \tilde{E}_k a_{\mathbf{k}}^* a_{\mathbf{k}} + \frac{g}{2} \sum_{\mathbf{r}} dV \psi^*(\mathbf{r}) \psi^*(\mathbf{r}) \psi(\mathbf{r}) \psi(\mathbf{r}), \quad (4)$$

where $\tilde{E}_k$ is the dispersion relation of the noninteracting waves, and the binary interaction between particles in the real gas is reflected in the classical field model by a field self-interaction with a coupling constant

$$g = \frac{4\pi\hbar^2 a}{m}, \quad (5)$$

where a is the s-wave scattering length of two atoms.

As a matter of a fact we use here the same refinement as in [13] consisting of modifying the dispersion relation in order to obtain for the ideal gas the correct quantum values of the mean occupation numbers at equipartition

$$\frac{1}{e^{\beta\hbar^2 k^2/2m} - 1} = \frac{k_B T}{\tilde{E}_k}. \quad (6)$$

However, we do not expect this to have a large impact here as we put a cutoff at an energy of the order of $k_B T$. More precisely we choose the number of the lattice points in a temperature dependent way, such that the maximal Bogoliubov energy on the lattice is equal to $k_B T$:

$$\max_{\mathbf{k}}[(\hbar^2 k^2/2m)(2\rho g + \hbar^2 k^2/2m)]^{1/2} = k_B T. \quad (7)$$

The discretized field has the following Poisson brackets:

$$i\hbar\{\psi(\mathbf{r}_1), \psi^*(\mathbf{r}_2)\} = \frac{\delta_{\mathbf{r}_1,\mathbf{r}_2}}{dV}, \quad (8)$$

where the Poisson brackets are such that $df/dt = \{f, H\}$ for a time-independent functional f of the field ψ. The field then evolves according to the nonlinear equation [26]

$$i\hbar\partial_t \psi = \left\{ k_B T \left[\exp\left(-\beta \frac{\hbar^2}{2m} \Delta \right) - 1 \right] + g|\psi(\mathbf{r},t)|^2 \right\} \psi. \quad (9)$$

We introduce the density and the phase of the condensate mode

$$a_0 = e^{i\theta} \sqrt{N_0}. \quad (10)$$

The quantity of interest is the variance of the condensate phase change during t:

$$\mathrm{Var}\ \varphi(t) = \langle \varphi(t)^2 \rangle - \langle \varphi(t) \rangle^2, \quad (11)$$

where

$$\varphi(t) = \theta(t) - \theta(0). \quad (12)$$

The averages are taken over stochastic realizations of the classical field, as the initial field samples the microcanonical ensemble with an energy E. For convenience, we parametrize the microcanonical ensemble by the temperature T such that the mean energy of the field in the canonical ensemble at temperature T is equal to E.

To generate the stochastic initial values of the classical field we proceed as follows. (i) First we generate 1000 stochastic fields in the canonical ensemble at temperature T, as explained in [13], and we compute the average energy of the field $\langle E \rangle_{\mathrm{can}}$ and its root-mean-squared fluctuations $\sigma = \sqrt{\mathrm{Var}\, E}$. (ii) We generate other fields, still in the canonical ensemble, and we filter them keeping only realizations with an energy E such that $|E - \langle E \rangle_{\mathrm{can}}| \leq 0.01\sigma/2$. (iii) We let each field evolve for some time interval with the Eq. (9) to eliminate transients due to the fact that the Bogoliubov approximation, used in the sampling, does not produce an exactly stationary distribution. After this "thermalization" period we start calculating the relevant observables, as ψ evolves with the same equation (9). In practice this equation is integrated numerically with the fast Fourier transform (FFT) splitting technique. The relative error on conservation of energy in the simulation is at the level of $10^{-7} - 10^{-6}$. The ensemble of data reported here has required a CPU time of about 2 years on Intel Xeon Quad Core 3 GHz processors.

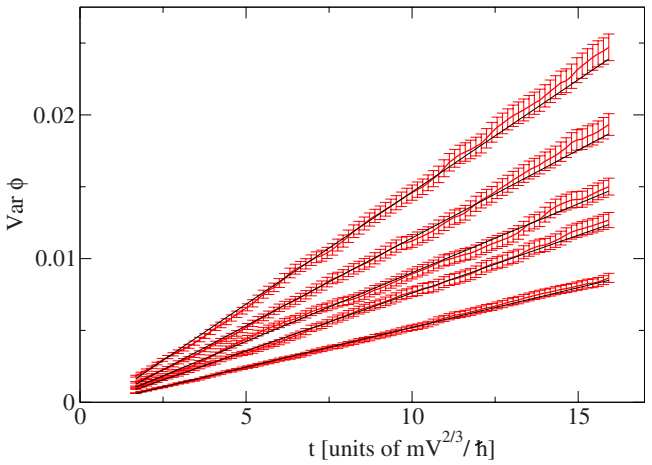

FIG. 1. (Color online) Variance of the condensate phase change $\varphi(t)$ as a function of time. Wavy line with error bars: numerical results. Solid lines: a linear fit. From bottom to top, the reduced temperature $k_B T/\rho g$ is 9.7, 13.2, 15.7, 19.6, and 24.2. The number of atoms is fixed to $N = 2.37 \times 10^6$. The high energy cutoff is fixed according to Eq. (7), on a grid 32^3, so that the temperature slightly varies, from bottom to top: $k_B T/(\hbar^2/mV^{2/3}) = 16\,864$, 16 411, 16 212, 16 010, and 15 854. The time is in units of $mV^{2/3}/\hbar$.

III. NUMERICAL RESULTS AND SCALING LAWS

The first important result that we obtain is the diffusive behavior of the condensate phase. In Fig. 1 we show an example of numerical data for Var $\varphi(t)$. From bottom to top, five values of $k_B T/\rho g$ are presented for a constant number of atoms $N = 2.36 \times 10^6$. The wavy line with error bars is the phase variance as a function of time obtained with about 1200 stochastic realizations [27]. The solid line is a linear fit from which we deduce the value of the diffusion coefficient,

$$\mathrm{Var}\ \varphi(t) \overset{t\to\infty}{\sim} 2Dt. \quad (13)$$

In Fig. 2 we show a histogram representing the probability distribution for the condensate phase change at the final time of the simulation for one of the curves in Fig. 1. The Gaussian distribution expected for a diffusive motion is also represented for comparison and remarkably agrees with the simulation results.

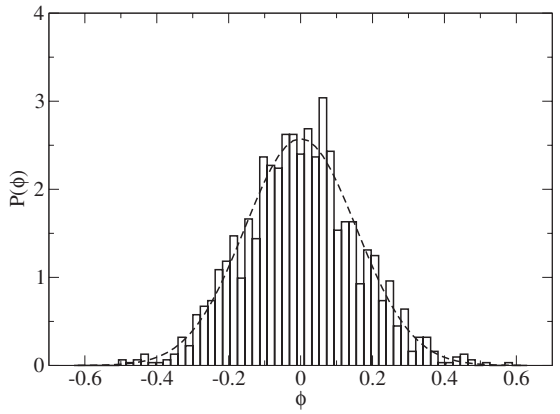

FIG. 2. Probability distribution for the condensate phase change between time $t=0$ and time $t=16\,mV^{2/3}/\hbar$. Histogram: Classical field simulation obtained with 1200 stochastic realizations for the parameters corresponding to the curve in Fig. 1 with the highest ratio of $k_BT/\rho g$: $k_BT=15\,854\hbar^2/(mV^{2/3})$, $N=2.37\times10^6$ on a 32^3 grid. Dashed line: Gaussian probability distribution expected for a diffusive motion of the phase with a diffusion coefficient $D=0.781\times10^{-3}\hbar/mV^{2/3}$ extracted from the linear fit in Fig. 1.

The diffusive behavior of the condensate phase is strictly related to the long time behavior of the time correlation function $\mathcal{C}$ of the condensate phase derivative $\dot{\varphi}$,

$$\mathcal{C}(|t'-t''|)=\langle\dot{\varphi}(t')\dot{\varphi}(t'')\rangle-\langle\dot{\varphi}(t')\rangle\langle\dot{\varphi}(t'')\rangle, \tag{14}$$

where we used the fact that $\mathcal{C}$ depends only on $|t'-t''|$ for a steady state classical field. By writing $\varphi(t)$ in terms of its time derivative, one obtains [13]

$$\mathrm{Var}\,\varphi(t)=2t\int_0^t d\tau\mathcal{C}(\tau)-2\int_0^t d\tau\tau\mathcal{C}(\tau). \tag{15}$$

If $\mathcal{C}(t)$ has a nonzero limit at long times, as it was the case in the canonical ensemble [13], Var φ grows quadratically in time. Here, in the microcanonical ensemble Var φ grows linearly in time and we expect that $\mathcal{C}(t)\to0$ when $t\to\infty$. An illustration of that, for two values of the temperature, is given in Fig. 3 where, for convenience, $\mathcal{C}(t)$ is calculated with a simplified formula for the phase derivative [28]

$$\hbar\dot{\varphi}\simeq-\rho g-\frac{g}{V}\sum_{\mathbf{k}\neq\mathbf{0}}(\tilde{U}_k+\tilde{V}_k)^2|b_{\mathbf{k}}|^2. \tag{16}$$

In Eq. (16) the $b_{\mathbf{k}}$ are the field amplitudes on the Bogoliubov modes [29].

We now investigate numerically how the diffusion coefficient scales in different limits. First we consider the "Bogoliubov limit" introduced in [30],

$$N\to\infty,\quad g\to0\quad\text{with } Ng=\text{const}, \tag{17}$$

the other parameters (V,l_1,l_2,l_3,T) being fixed [31]. In this limit, the number of noncondensed particles converges to a nonzero value while the noncondensed fraction vanishes. The time evolution of the Bogoliubov occupation numbers $n_{\mathbf{k}}=|b_{\mathbf{k}}|^2$ is then mainly due to terms in the interaction Hamiltonian which are cubic in the noncondensed field amplitude and linear in the condensate amplitude and thus of order $\epsilon=g\sqrt{N}$. Physically these cubic terms describe interactions among Bogoliubov modes such as Landau and Beliaev processes [32–35], which are included in the classical field model [19–22,36–40,42]. They lead to evolution rates of the $n_{\mathbf{k}}$ of order ϵ^2. We thus expect a phase diffusion coefficient of the same order ϵ^2, which is $\propto1/N$ according to Eq. (17). This expectation is confirmed numerically as we show in Fig. 4, where we find that DN is constant within the error bars over a factor of 5 variation of N and for three considered temperatures.

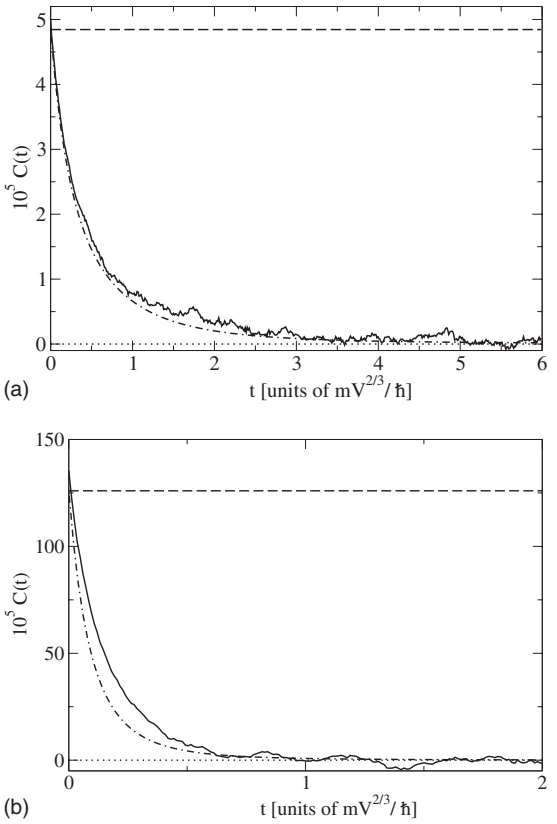

FIG. 3. Correlation function $\mathcal{C}(t)$ of the phase derivative $\dot{\varphi}(t)$ given by the nonoscillating approximation (16), as a function of time. Solid line: numerical results. Dashed line: result of Bogoliubov theory. Dashed-dotted line: prediction of the projected Gaussian approach of Sec. IV. The number of atoms is fixed to $N=5\times10^6$, and the Gross-Pitaevskii chemical potential is fixed to $\rho g=700\hbar^2/mV^{2/3}$. In (a) the temperature is $k_BT/(\hbar^2/mV^{2/3})=5469$, with a grid size 18^3. In (b) the temperature is $k_BT/(\hbar^2/mV^{2/3})=14\,054$, with a grid size 30^3. $C(t)$ is in units of $\hbar^2/mV^{2/3}$.

We now investigate the existence of a thermodynamical limit for the quantity DN, given that the Bogoliubov limit is already reached. The thermodynamical limit is defined as usual as

$$N\to\infty,\quad V\to\infty\quad\text{with } \rho=\text{const}, \tag{18}$$

the other parameters (g,l_1,l_2,l_3,T) being fixed. The result is shown in Fig. 5 where DN is constant within the error bars, over a factor of 5 of variation of N and four considered values of $k_BT/\rho g$.

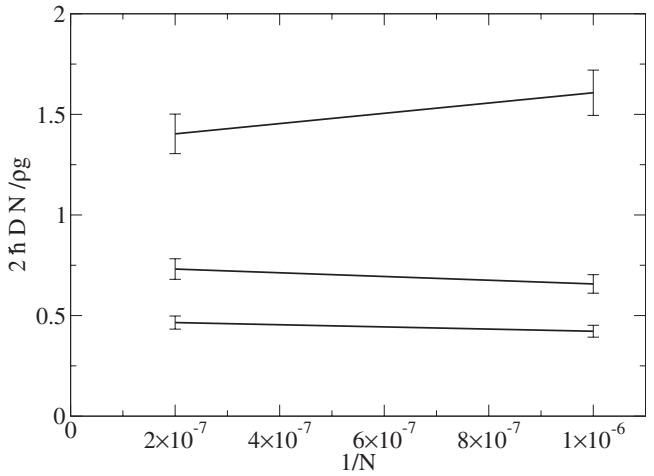

FIG. 4. Scaling of the phase diffusion coefficient in the Bogoliubov limit (17), for a factor of 5 variation of the atom number N. The Gross-Pitaevskii chemical potential is fixed to $\rho g = 700\hbar^2/mV^{2/3}$. Points with error bars: Simulation results. The lines connect the points with the same temperature. From bottom to top: $k_BT = 5469\hbar^2/mV^{2/3}$ with a grid size 18^3, $k_BT = 6606\hbar^2/mV^{2/3}$ with a grid size 20^3, and $k_BT = 9231\hbar^2/mV^{2/3}$ with a grid size 24^3.

In what follows, using dimensional analysis, we show that for our cutoff procedure (7), the dimensionless quantity $\hbar DN/\rho g$ is a function of a single parameter $k_BT/\rho g$ once the Bogoliubov and thermodynamical limits are reached. Six independent physical quantities are present in the model,

$$\{\hbar, m, g, V, k_BT, N\}. \tag{19}$$

The lattice spacings l_1, l_2, l_3 are not independent parameters since their ratios are fixed and their value is determined by Eq. (7) once the quantities (19) are fixed. Equivalently we can replace g by ρg and the volume V by k_BT_c, where T_c is

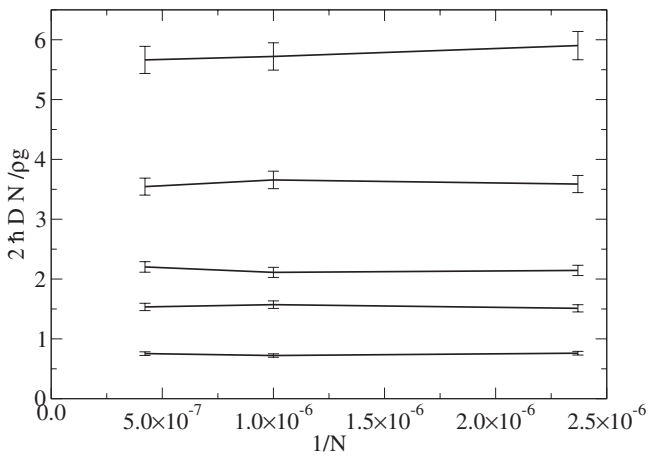

FIG. 5. Scaling of the phase diffusion coefficient in the thermodynamic limit (18), for a factor of 5 variation of the atom number N. Points with error bars: simulation results. The lines connect the points with the same $k_BT/\rho g$. The points most on the left of the figure, with $N = 2.37 \times 10^6$, are the ones of Fig. 1, with a grid size 32^3. The other points are for a grid size 24^3 ($N = 10^6$) and for a grid size 18^3 ($N = 4.22 \times 10^5$).

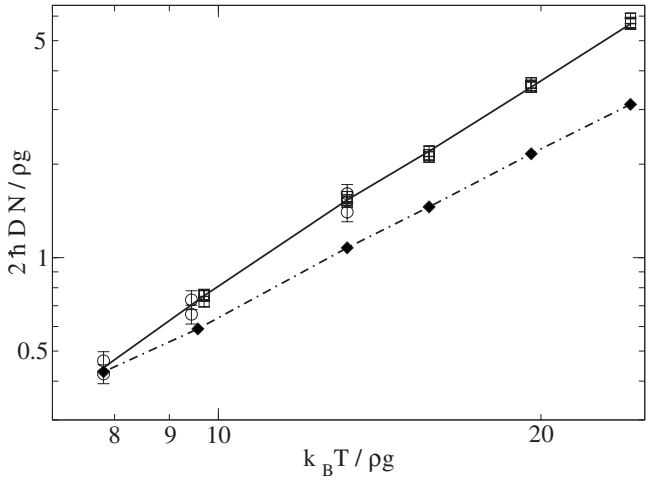

FIG. 6. Universal curve for the rescaled phase diffusion coefficient as a function of $k_BT/\rho g$ in log-log scale. Symbols with error bars: simulation results. Circles: results of Fig. 4. Squares: results of Fig. 5. The solid line connects the points with the largest value of N of Fig. 5, plus the average of the two points of Fig. 4 with the lowest temperature. Dashed-dotted line with filled diamonds: D^{approx} from the projected Gaussian approach. The $\Gamma_{\mathbf{k}}$ for the projected Gaussian approach are calculated on the grids used in the simulations corresponding to the points connected by the solid line.

the transition temperature of the ideal gas given by

$$\rho\left(\frac{2\pi\hbar^2}{mk_BT_c}\right)^{3/2} = \zeta(3/2). \tag{20}$$

We then have

$$\frac{\hbar DN}{\rho g} = f\left(\hbar, m, \rho g, \frac{k_BT_c}{\rho g}, \frac{k_BT}{\rho g}, N\right). \tag{21}$$

The three quantities $\hbar$, m, and ρg can be recombined to form a length, a time, and a mass which are three independent dimensioned quantities. Since f and its other three variables are dimensionless, f does not depend of its first three variables. In the thermodynamical limit, N tends to infinity so the sixth variable of f drops out of the problem. In the Bogoliubov limit, $k_BT_c/\rho g \to \infty$ so that the forth variable of f also drops. We thus conclude that

$$\frac{\hbar DN}{\rho g} = f\left(\frac{k_BT}{\rho g}\right). \tag{22}$$

In Fig. 6 we show the graph of f as obtained by our classical field model collecting all the simulation results of Figs. 5 and 4. We have used a log-log scale in Fig. 6 to reveal that the function f is approximately a power law in the considered range of $k_BT/\rho g$.

IV. PROJECTED GAUSSIAN APPROXIMATION

In this section we propose an approximate analytical formula for the phase diffusion coefficient that gives some physical insight and can be extended to the quantum field case.

A. Classical field

We wish to calculate the integral of a correlation function $\mathcal{C}(t)=\langle A(t)A(0)\rangle-\langle A(t)\rangle\langle A(0)\rangle$ of an observable A of the form

$$A=\sum_{\mathbf{k}\neq\mathbf{0}} A_{\mathbf{k}}|b_{\mathbf{k}}|^2, \tag{23}$$

where $b_{\mathbf{k}}$ are the amplitudes of the field over the Bogoliubov modes. We thus introduce the $\mathcal{M}\times\mathcal{M}$ covariance matrix Q with matrix elements

$$Q_{\mathbf{k},\mathbf{k}'}(t)=\langle \delta n_{\mathbf{k}}(t)\delta n_{\mathbf{k}'}(0)\rangle, \tag{24}$$

where $\delta n_{\mathbf{k}}=n_{\mathbf{k}}-\bar{n}_k$ is the fluctuation of the occupation number of the corresponding Bogoliubov mode and $\mathcal{M}=V/(l_1l_2l_3)-1$ is the number of Bogoliubov modes. One thus has

$$\mathcal{C}(t)=\vec{A}\cdot Q(t)\vec{A}, \tag{25}$$

where $\vec{A}$ is the vector of components $A_{\mathbf{k}}$. Since the system is described in this section by the microcanonical ensemble for the Bogoliubov Hamiltonian, the matrix Q obeys the relation

$$\vec{\epsilon}\cdot Q\vec{X}=0\ \forall\ \vec{X},\quad \text{and } Q\vec{\epsilon}=\vec{0}, \tag{26}$$

where the vector $\vec{\epsilon}$ collects the Bogoliubov energies $\tilde{\epsilon}_k$.

By using the microcanonical classical field averages [41] one directly accesses the $t=0$ value of the matrix Q,

$$\text{for } \mathbf{k}\neq\mathbf{k}':\quad Q_{\mathbf{k},\mathbf{k}'}(0)=-\frac{\bar{n}_k\bar{n}_{k'}}{\mathcal{M}+1}, \tag{27}$$

$$\text{for } \mathbf{k}=\mathbf{k}':\quad Q_{\mathbf{k},\mathbf{k}}(0)=\bar{n}_k^2\frac{\mathcal{M}-1}{\mathcal{M}+1}, \tag{28}$$

where the $\bar{n}_k=k_BT/\tilde{\epsilon}_k$ are the classical field occupation numbers. Remarkably we can express this result in terms of the result one would have in the canonical ensemble with average energy equal to the microcanonical energy, adding a projector which suppresses energy fluctuations:

$$Q(0)=\frac{\mathcal{M}}{\mathcal{M}+1}P^{\dagger}Q^{\text{Gauss}}(0)P \tag{29}$$

with

$$P_{\mathbf{k},\mathbf{k}'}=\delta_{\mathbf{k},\mathbf{k}'}-\tilde{\epsilon}_{\mathbf{k}}\alpha_{\mathbf{k}'}. \tag{30}$$

The vector $\vec{\alpha}$ is adjoint to the vector $\vec{\epsilon}$ so that $P\vec{\epsilon}=\vec{0}$. Its components are given by

$$\alpha_{\mathbf{k}}=\frac{1}{\mathcal{M}\tilde{\epsilon}_{\mathbf{k}}} \tag{31}$$

and Q^{Gauss} is the value of the covariance matrix in the canonical ensemble

$$Q^{\text{Gauss}}_{\mathbf{k},\mathbf{k}'}(0)=\delta_{\mathbf{k},\mathbf{k}'}\bar{n}_k^2. \tag{32}$$

The apex "Gauss" recalls the fact that the $b_{\mathbf{k}}$ have a Gaussian probability distribution in the canonical ensemble, contrarily to the case of the microcanonical ensemble.

For the $t=0$ value of the phase derivative correlation function one then obtains

$$\mathcal{C}(0)=\frac{\mathcal{M}}{\mathcal{M}+1}\left[\sum_{\mathbf{k}\neq\mathbf{0}}A_{\mathbf{k}}^2\bar{n}_k^2-\frac{1}{\mathcal{M}}\left(\sum_{\mathbf{k}\neq\mathbf{0}}A_{\mathbf{k}}\bar{n}_k\right)^2\right] \tag{33}$$

with

$$A_{\mathbf{k}}=-\frac{g}{V}(\tilde{U}_k+\tilde{V}_k)^2. \tag{34}$$

We verified that Eq. (33), represented as a dashed line in Fig. 3, is in agreement with the numerical simulation as one enters the Bogoliubov limit (17). Note that within the Bogoliubov aproximation $b_{\mathbf{k}}(t)\simeq b_{\mathbf{k}}(0)e^{-i\tilde{\epsilon}_kt/\hbar}$, the phase derivative correlation function remains equal to its $t=0$ value (33) at all times. This is in clear disagreement with the numerical simulation, and it would lead to a ballistic spreading of the condensate phase.

Our approximate treatment consists of extending the relation (29) to positive times, using the fact that in a Gaussian theory one would have

$$Q^{\text{Gauss}}_{\mathbf{k},\mathbf{k}'}(t)=Q^{\text{Gauss}}_{\mathbf{k},\mathbf{k}'}(0)e^{-\Gamma_{\mathbf{k}}t}. \tag{35}$$

One indeed assumes in the Gaussian model

$$|\langle b^*_{\mathbf{k}}(t)b_{\mathbf{k}'}(0)\rangle_{\text{Gauss}}|=\delta_{\mathbf{k},\mathbf{k}'}\bar{n}_ke^{-\Gamma_{\mathbf{k}}t/2} \tag{36}$$

and one uses Wick theorem to obtain Eq. (35). Physically Eq. (36) describes Beliaev-Landau processes that decorrelate the $b_{\mathbf{k}}$. It can be derived, for example, with a master equation approach as done in an appendix of [13].

For the phase derivative correlation function one then obtains the approximate expression

$$\mathcal{C}^{\text{approx}}(t)=\frac{\mathcal{M}}{\mathcal{M}+1}\left[\sum_{\mathbf{k}\neq\mathbf{0}}A_{\mathbf{k}}^2\bar{n}_k^2e^{-\Gamma_{\mathbf{k}}t}-\frac{2}{\mathcal{M}}\left(\sum_{\mathbf{k}\neq\mathbf{0}}A_{\mathbf{k}}\bar{n}_k\right)\times\left(\sum_{\mathbf{k}'\neq\mathbf{0}}A_{\mathbf{k}'}\bar{n}_{k'}e^{-\Gamma_{\mathbf{k}'}t}\right)+\frac{1}{\mathcal{M}^2}\left(\sum_{\mathbf{q}\neq\mathbf{0}}e^{-\Gamma_qt}\right)\times\left(\sum_{\mathbf{k}\neq\mathbf{0}}A_{\mathbf{k}}\bar{n}_k\right)^2\right]. \tag{37}$$

We represent Eq. (37) as a dashed-dotted line in Fig. 3. The resulting approximation on the diffusion coefficient is obtained by integration

$$D^{\text{approx}}=\int_0^{+\infty}\mathcal{C}^{\text{approx}}(t)dt. \tag{38}$$

In Fig. 6 we compare the approximation (38) (diamonds linked by a dashed-dotted line) to the numerical simulation results. The agreement is acceptable in the considered range of $k_BT/\rho g$. The Beliaev-Landau damping rates $\Gamma_{\mathbf{k}}$ are calculated on the same discrete grid as the simulation points as explained in [42].

B. Quantum field

In this section we extend the approximate formula for the phase diffusion coefficient to the quantum case. The Bogo-

liubov amplitudes and occupation numbers are now operators $\hat{b}_{\mathbf{k}}$, $\hat{n}_{\mathbf{k}}$. As in the classical field case we introduce the covariance matrix of the Bogoliubov occupation numbers

$$Q_{\mathbf{k},\mathbf{k}'}(t) = \langle \delta\hat{n}_{\mathbf{k}}(t)\delta\hat{n}_{\mathbf{k}'}(0)\rangle. \tag{39}$$

To obtain the $t=0$ value of Q we need to compute quantum averages in the microcanonical ensemble. To this end we use a result derived in [13] giving the first deviation between the microcanonical expectation value $\langle O\rangle$ and the canonical one $\langle O\rangle_{\text{can}}(T)$ in the limit of a large system for an arbitrary observable O:

$$\langle O\rangle - \langle O\rangle_{\text{can}}(T) \simeq -\frac{1}{2}k_B T^2 \frac{d}{dT}\left(\frac{d\langle O\rangle_{\text{can}}/dT}{d\langle H\rangle_{\text{can}}/dT}\right), \tag{40}$$

where the canonical temperature T is such that the mean energy $\langle H\rangle_{\text{can}}$ in the canonical ensemble is equal to the microcanonical energy E.

For $\mathbf{k}\neq\mathbf{k}'$, using $d\bar{n}_k/dT = \epsilon_k \bar{n}_k(\bar{n}_k+1)/k_B T^2$, one finds

$$Q_{\mathbf{k},\mathbf{k}'}(0) \simeq -\frac{\epsilon_k \epsilon_{k'} \bar{n}_k(\bar{n}_k+1)\bar{n}_{k'}(\bar{n}_{k'}+1)}{\Sigma_{\mathbf{q}\neq\mathbf{0}}\epsilon_q^2 \bar{n}_q(\bar{n}_q+1)}, \tag{41}$$

where the $\bar{n}_k = 1/[\exp(\beta\epsilon_k)-1]$ are the quantum occupation numbers. This scales as $1/\mathcal{M}$ in the thermodynamic limit. Since the number of off-diagonal terms of Q in Eq. (25) is about $\mathcal{M}$ times larger than the number of diagonal terms of Q, we have for consistency to calculate the diagonal terms of Q up to order $1/\mathcal{M}^0$, that is the deviation from the canonical value $\bar{n}_k(\bar{n}_k+1)$ is not required. To exactly obtain the energy conservation (26), it is, however, convenient to include, rather than the exact deviation between the canonical and microcanonical values, an *ad hoc* approximate correction of order $1/\mathcal{M}$:

$$Q_{\mathbf{k},\mathbf{k}} \simeq \bar{n}_k(\bar{n}_k+1) - \frac{\epsilon_k^2 \bar{n}_k^2(\bar{n}_k+1)^2}{\Sigma_{\mathbf{q}\neq\mathbf{0}}\epsilon_q^2 \bar{n}_q(\bar{n}_q+1)}. \tag{42}$$

In this way, we recover the structure of Eq. (29), where the $t=0$ value of Q is deduced from the one in the canonical ensemble,

$$Q^{\text{Gauss}}_{\mathbf{k},\mathbf{k}'}(t=0) = \bar{n}_k(\bar{n}_k+1)\delta_{\mathbf{k},\mathbf{k}'} \tag{43}$$

by the action of a projector P,

$$Q(t=0) \simeq P^\dagger Q^{\text{Gauss}}(t=0)P. \tag{44}$$

The projector P still involves the dyadic structure (30),

$$P_{\mathbf{k},\mathbf{k}'} = \delta_{\mathbf{k},\mathbf{k}'} - \epsilon_{\mathbf{k}}\alpha_{\mathbf{k}'}, \tag{45}$$

with a new expression for the vector $\vec{\alpha}$:

$$\alpha_{\mathbf{k}} = \frac{\epsilon_k \bar{n}_k(\bar{n}_k+1)}{\Sigma_{\mathbf{q}\neq\mathbf{0}}\epsilon_q^2 \bar{n}_q(\bar{n}_q+1)}. \tag{46}$$

As a check, one can apply the classical field limit to the above quantum expressions. One recovers Eq. (29), apart from the global factor $\mathcal{M}/(\mathcal{M}+1)$, whose deviation from unity gives rise to terms beyond the accuracy of the present calculation.

At positive times, our quantum projected Gaussian approximation assumes that Eq. (44) still holds,

$$Q^{\text{approx}}(t) \simeq P^\dagger Q^{\text{Gauss}}(t)P \tag{47}$$

with the Gaussian covariance matrix

$$Q^{\text{Gauss}}_{\mathbf{k},\mathbf{k}'}(t) = \delta_{\mathbf{k},\mathbf{k}'}\bar{n}_k(\bar{n}_k+1)e^{-\Gamma_{\mathbf{k}}t}, \tag{48}$$

where the Beliaev-Landau damping rate $\Gamma_{\mathbf{k}}$ is now the usual one, that is for the quantum field theory. From the quantum equivalent of Eq. (25) one obtains an approximate expression for the phase derivative correlation function, and from the quantum equivalent of Eq. (38) an approximate expression for the quantum field phase diffusion coefficient [43]:

$$D^{\text{approx}} = \sum_{\mathbf{k}\neq\mathbf{0}} [(P\vec{A})_{\mathbf{k}}]^2 \frac{\bar{n}_k(\bar{n}_k+1)}{\Gamma_{\mathbf{k}}}, \tag{49}$$

where the projection of the vector $\vec{A}$ was introduced:

$$(P\vec{A})_{\mathbf{k}} = -\frac{g}{V}\times\left[(U_k+V_k)^2 - \epsilon_k \frac{\Sigma_{\mathbf{q}\neq\mathbf{0}}\epsilon_q(U_q+V_q)^2\bar{n}_q(\bar{n}_q+1)}{\Sigma_{\mathbf{q}\neq\mathbf{0}}\epsilon_q^2\bar{n}_q(\bar{n}_q+1)}\right] \tag{50}$$

with

$$A_{\mathbf{k}} = -\frac{g}{V}(U_k+V_k)^2. \tag{51}$$

In this expression, the modes amplitudes U_k, V_k and energy ϵ_k have the usual expressions of the quantum field Bogoliubov theory,

$$U_k+V_k = \frac{1}{U_k-V_k} = \left(\frac{\hbar^2k^2/2m}{2\rho g+\hbar^2k^2/2m}\right)^{1/4}, \tag{52}$$

$$\epsilon_k = \left[\frac{\hbar^2k^2}{2m}\left(2\rho g+\frac{\hbar^2k^2}{2m}\right)\right]^{1/2}. \tag{53}$$

In Appendix A we give the explicit expression of the Beliaev-Landau damping rates Γ_k and the approximate phase diffusion coefficient in the thermodynamic limit. The existence of such a limit is due to the fact that none of the momentum integrals involved are infrared divergent, keeping in mind that $(U_k+V_k)^2$, ϵ_k, and Γ_k vanish linearly with k [34], while $\bar{n}_k(\bar{n}_k+1)$ diverges as $1/k^2$. As expected from the analysis of the previous section, the scaled diffusion coefficient $\hbar D^{\text{approx}}N/\rho g$ is a function of $k_BT/\rho g$ only, see Eq. (A16).

In Fig. 7 we show the values of D^{approx} for the quantum field in the thermodynamic limit for the same values of $k_BT/\rho g$ as in Fig. 6. To see the effect of an energy truncation at k_BT, we also show the values of D^{approx} obtained by introducing an energy cutoff $\epsilon_q < k_BT$ in Eq. (A16) and the same cutoff $\epsilon_k < k_BT$ in the integrals (A1) and (A9) giving the damping rate Γ_q. As expected, the resulting values of D^{approx} are close to the values of D^{approx} obtained for the classical field model in Fig. 6, and that we have reported in Fig. 7 for comparison. We conclude that the diffusion coefficient is indeed affected by an energy cutoff, and the coefficient obtained in the classical field simulations with an energy cutoff

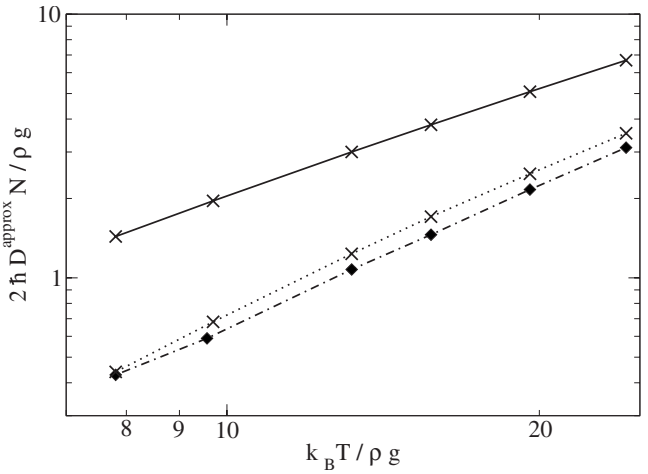

FIG. 7. Approximate phase diffusion coefficient for the quantum field in the thermodynamic limit as a function of $k_B T/\rho g$ in log-log scale. Solid line with crosses: D^{approx} for the quantum field from Eq. (A16). Dotted line with crosses: effect of an energy cutoff equal to $k_B T$ in Eq. (A16). Dashed-dotted line with filled diamonds: D^{approx} for the classical field from Eq. (38) for finite size grids (data already shown as filled diamonds in Fig. 6).

$k_B T$ might differ quantitatively from the real one by a factor as much as 2, in the considered range of values of $k_B T/\rho g$.

V. CONCLUSION

Using a classical field model, we have shown that the phase of a uniform Bose-Einstein condensate undergoes true diffusion in time, when the gas is initially prepared in the microcanonical ensemble. Parametrizing the microcanonical energy E by the temperature T of the canonical ensemble with average energy E, we could show that the rescaled diffusion coefficient $\hbar DN/\rho g$, where N is the fixed number of particles and ρg is the Gross-Pitaevskii chemical potential, is a function of a single variable $k_B T/\rho g$ in the double thermodynamic and Bogoliubov limit.

We have derived an approximate formula for the diffusion coefficient, in fair agreement with the classical field simulations. We have generalized the approximate formula to the quantum field case, showing that it also admits a thermodynamic limit and that it satisfies the scaling property found for the classical field. We have used the quantum approximate formula to evaluate the effect of an energy cutoff, not required in the quantum theory and unavoidable in the classical field model.

The perspective of using the condensate phase spreading to experimentally distinguish among different statistical ensembles is fascinating, although the measurement of the intrinsic phase diffusion of a Bose-Einstein condensate discussed here remains a challenge and will be the subject of further investigations.

ACKNOWLEDGMENTS

The authors would like to thank E. Witkowska for her initial contribution to the project, K. Mølmer for hospitality and useful discussions, and F. Hulin-Hubard for valuable help with computers. A.S. acknowledges stimulating discussions with W. Phillips, K. Rzążewski, M. Gajda, and M. Oberthaler. We acknowledge financial support from IFRAF (Institut Francilien de Recherche sur les Atomes Froids).

APPENDIX A: BELIAEV-LANDAU DAMPING RATES AND APPROXIMATE PHASE DIFFUSION COEFFICIENT IN THE THERMODYNAMIC LIMIT

We start with the Landau damping rate of a Bogoliubov mode of wave vector $\mathbf{q}$ as given in [13],

$$\Gamma_q^L = \frac{g^2\rho}{\pi^2\hbar}\int d^3k L_{k,k'}^2(\bar{n}_k - \bar{n}_{k'})\,\delta(\epsilon_q + \epsilon_k - \epsilon_{k'}) \tag{A1}$$

with

$$L_{k,k'} = U_q V_k U_{k'} + (U_q + V_q)(U_k U_{k'} + V_k V_{k'}) + V_q U_k V_{k'}. \tag{A2}$$

The mode of wave vector $\mathbf{q}$ scatters an excitation of wave vector $\mathbf{k}$ giving rise to an excitation of wave vector $\mathbf{k}'$. The final mode has to satisfy momentum conservation so that $\mathbf{k}'=\mathbf{k}+\mathbf{q}$. Energy conservation $\epsilon_q+\epsilon_k=\epsilon_{k'}$ is ensured by the delta distribution in Eq. (A1). In the integral over $\mathbf{k}$ we use spherical coordinates of axis $\mathbf{q}$, θ being the polar angle. We introduce the momentum $\check{q}$ scaled by the inverse of the healing length ξ and the mode energy $\check{\epsilon}_q$ scaled by the Gross-Pitaevskii chemical potential ρg:

$$\check{q} = q\left(\frac{\hbar^2}{2m\rho g}\right)^{1/2} = q\xi, \tag{A3}$$

$$\check{\epsilon}_q = \frac{\epsilon_q}{\rho g} = [\check{q}^2(\check{q}^2+2)]^{1/2}. \tag{A4}$$

As a consequence, the mean occupation number $\bar{n}_q$ is a function of $\check{q}$ and of the ratio $k_B T/\rho g$ only, and the mode amplitudes U_q, V_q are functions of $\check{q}$ only. Introducing the notation $u=\cos\theta$, one has

$$\delta(\check{\epsilon}_q + \check{\epsilon}_k - \check{\epsilon}_{k'}) = \delta(u - u_0^L)\frac{\check{\epsilon}_q + \check{\epsilon}_k}{2\check{k}\check{q}[1+(\check{\epsilon}_q+\check{\epsilon}_k)^2]^{1/2}}, \tag{A5}$$

where

$$u_0^L = \frac{[1+(\check{\epsilon}_q+\check{\epsilon}_k)^2]^{1/2} - (1+\check{q}^2+\check{k}^2)}{2\check{k}\check{q}}. \tag{A6}$$

One can show that u_0^L is in between -1 and 1 for all values of $\check{k}$ and $\check{q}$, so that the angular integration is straightforward and leads to

$$\Gamma_q^L = \frac{g}{\pi\hbar\xi^3}\int_0^{+\infty} d\check{k} L_{k,k'}^2 \frac{\check{k}(\check{\epsilon}_k + \check{\epsilon}_q)(\bar{n}_k - \bar{n}_{k'})}{\check{q}[1+(\check{\epsilon}_q+\check{\epsilon}_k)^2]^{1/2}} \tag{A7}$$

with

$$1 + \check{k}'^2 = [1+(\check{\epsilon}_q+\check{\epsilon}_k)^2]^{1/2}. \tag{A8}$$

A similar procedure may be applied to the Beliaev damping rate for the mode **q**. From [13] one has

$$\Gamma_q^B = \frac{g^2\rho}{2\pi^2\hbar}\int d^3k B_{k,k'}^2(1+\bar{n}_k+\bar{n}_{k'})\delta(\epsilon_k+\epsilon_{k'}-\epsilon_q) \tag{A9}$$

with

$$B_{k,k'} = U_qU_kU_{k'} + (U_q+V_q)(V_kU_{k'}+U_kV_{k'}) + V_qV_kV_{k'}. \tag{A10}$$

Here the mode of wave vector **q** decays into an excitation of wave vector **k** and an excitation of wave vector **k**′. Momentum conservation imposes $\mathbf{k}'=\mathbf{q}-\mathbf{k}$. Energy conservation $\epsilon_{k'}=\epsilon_q-\epsilon_k$ is ensured by the delta distribution in Eq. (A9), and clearly imposes $k<q$. With the same scaled variables and spherical coordinates as above, one obtains

$$\delta(\check{\epsilon}_k+\check{\epsilon}_{k'}-\check{\epsilon}_q) = \delta(u-u_0^B)\frac{\check{\epsilon}_q-\check{\epsilon}_k}{2\check{k}\check{q}[1+(\check{\epsilon}_q-\check{\epsilon}_k)^2]^{1/2}}, \tag{A11}$$

where

$$u_0^B = \frac{1+\check{q}^2+\check{k}^2-[1+(\check{\epsilon}_q-\check{\epsilon}_k)^2]^{1/2}}{2\check{k}\check{q}}. \tag{A12}$$

One can show that u_0^B is in between −1 and 1, whatever the values of $\check{q}$ and $\check{k}<\check{q}$, so that angular integration is straightforward and gives

$$\Gamma_q^B = \frac{g}{2\pi\hbar\xi^3}\int_0^{\check{q}} d\check{k}B_{k,k'}^2\frac{\check{k}(\check{\epsilon}_q-\check{\epsilon}_k)(1+\bar{n}_k+\bar{n}_{k'})}{\check{q}[1+(\check{\epsilon}_q-\check{\epsilon}_k)^2]^{1/2}} \tag{A13}$$

with

$$1+\check{k}'^2 = [1+(\check{\epsilon}_q-\check{\epsilon}_k)^2]^{1/2}. \tag{A14}$$

Finally we introduce the rescaled total damping rate,

$$\check{\Gamma}_q = \frac{2\pi^2\hbar\xi^3}{g}(\Gamma_q^L+\Gamma_q^B), \tag{A15}$$

a dimensionless function of $k_BT/\rho g$ only. From Eq. (49) one then obtains in the thermodynamic limit an approximate expression for the phase diffusion coefficient depending only on $k_BT/\rho g$,

$$\frac{\hbar D^{\text{approx}}N}{\rho g} = \int_0^{+\infty} d\check{q}\check{q}^2(\mathcal{A}_q^P)^2\frac{\bar{n}_q(1+\bar{n}_q)}{\check{\Gamma}_q} \tag{A16}$$

with

$$\mathcal{A}_q^P = (U_q+V_q)^2 - \check{\epsilon}_q\frac{\int_0^{+\infty}d\check{k}\check{k}^2\check{\epsilon}_k(U_k+V_k)^2\bar{n}_k(\bar{n}_k+1)}{\int_0^{+\infty}d\check{k}\check{k}^2\check{\epsilon}_k^2\bar{n}_k(\bar{n}_k+1)}. \tag{A17}$$

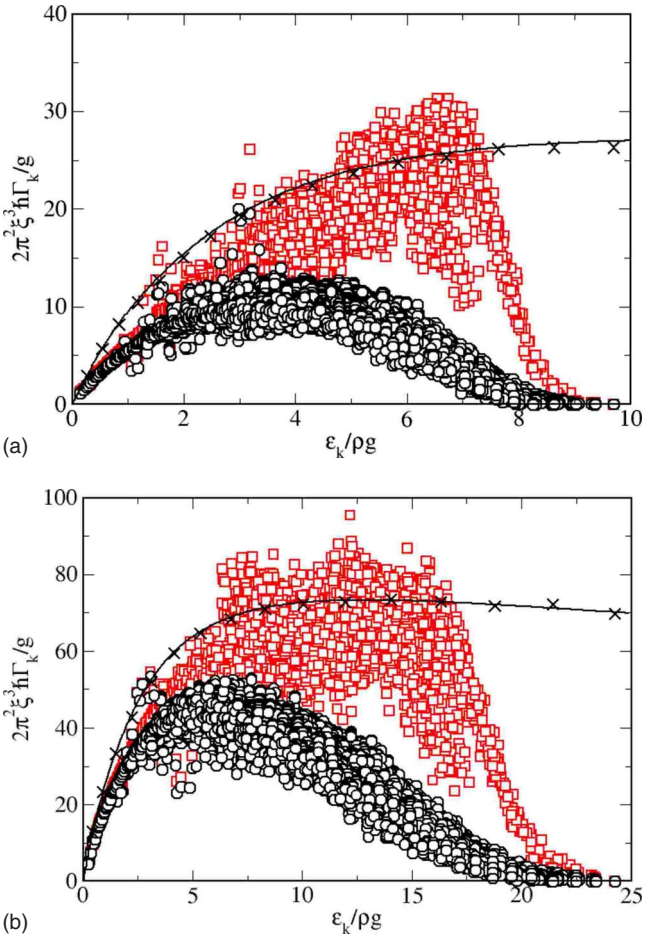

FIG. 8. (Color online) Beliaev-Landau damping rates $\Gamma_{\mathbf{k}}$ as functions of the quantum Bogoliubov energy ϵ_k of the modes in units of ρg. The damping rates are normalized as in Eq. (A15). Red squares: classical field model used in the present work (grid 32^3), including Umklapp processes. Black circles: classical field model without the Umklapp processes (grid 32^3). Crosses: quantum model with lattice spacings l_i reduced by a factor of 2 (grid 64^3); the displayed values of $\Gamma_{\mathbf{k}}$ are limited to modes on the diagonal of the numerical grid ($k_x=k_y=k_z>0$, with $\epsilon_k<k_BT$). Solid line: quantum result in the thermodynamic and quasicontinuous limit. Parameters: (a) $N=2.37\times10^6$, $k_BT/(\hbar^2/mV^{2/3})=16\,864$, $k_BT/\rho g=9.7$, corresponding to the lowest curve in Fig. 1. (b) $N=2.37\times10^6$, $k_BT/(\hbar^2/mV^{2/3})=15\,854$, $k_BT/\rho g=24.2$, corresponding to the highest curve in Fig. 1.

APPENDIX B: INFLUENCE OF UMKLAPP PROCESSES ON BELIAEV-LANDAU DAMPING RATES FOR THE CLASSICAL FIELD

As mentioned in [23], our lattice model Hamiltonian contains Umklapp processes, i.e., the interaction term when written in momentum space involves some scattering processes that do not conserve the total momentum (but they of course conserve it modulo $2\pi\hbar/l_i$ along direction i, where l_i is the lattice spacing along that direction). A real atomic gas in free space does not present such Umklapp processes. In a quantum theory, the use of a lattice model is legitimate in the quasicontinuous limit, as the lattice spacing becomes much smaller than the physical length scales of the gas such as the

healing length and the thermal de Broglie wavelength, while remaining larger than the scattering length to ensure that the interaction potential remains positive [44]. In our implementation of the classical field model one cannot take the quasicontinuous limit since an energy cutoff of order k_BT is intrinsically necessary, so that we expect an effect of the Umklapp processes on the dynamics.

To assess the importance of this effect, in this appendix we calculate the Beliaev-Landau damping rates $\Gamma_{\mathbf{k}}$ for two different lattice models, with and without Umklapp processes, and we compare them to the well-established quantum result in the thermodynamic limit.

In Fig. 8 we plot the Beliaev-Landau damping rates calculated using the perturbative method of [42] for all the Bogoliubov modes present in our numerical grid, as functions of the quantum Bogoliubov energy ϵ_k. The red squares are for the classical field model used in the present work, including Umklapp processes. The black circles are for a second classical field model, deduced from the first one by projecting out the Umklapp processes in the interaction term. The solid line is the quantum result in the thermodynamic limit. Note that the classical field damping rates calculated on the grid are spread over a large range of values for a given energy.

At low energy $\epsilon_k \ll k_BT$ the two classical field models (with and without Umklapp) agree. At higher energies the model with Umklapp processes gives larger rates which are closer to the quantum theory. The fact that the model without Umklapp processes gives lower damping rates is understandable as many scattering processes happening close to the cutoff region are inhibited. Finally, for $\epsilon_k \simeq k_BT$ in the corners of the numerical grid, both classical field models show small damping rates very far from quantum reality.

We thus conclude that for the parameters range we considered, and for our specific way of relating the grid spacing to the temperature, the classical model with Umklapp processes is actually preferable to the projected one, since it avoids the emergence of a large number of modes with an anomalously low damping rate.

As a consistency check, in Fig. 8 we also plot the results of a third model (crosses) which is the quantum version of our lattice model (with the usual quadratic dispersion relation $E_k = \hbar^2 k^2 / 2m$), on a larger grid: i.e., reducing the lattice spacings by a factor of 2 with respect to the classical field model for a fixed volume of the box. We see that these quantum damping rates, calculated only for the modes along the diagonal of the numerical grid $k_x = k_y = k_z > 0$, agree well with the prediction of the well-established Beliaev-Landau theory in the thermodynamic limit (solid line) exposed in Appendix A.

[1] K. Bongs and K. Sengstock, Rep. Prog. Phys. **67**, 907 (2004); T. Schumm, S. Hofferberth, L. M. Anderson, S. Wildermuth, S. Groth, I. Bar-Joseph, J. Schmiedmayer, and P. Krüger, Nat. Phys. **1**, 57 (2005); P. Treutlein, P. Hommelhoff, T. Steinmetz, T. W. Hänsch, and J. Reichel, Phys. Rev. Lett. **92**, 203005 (2004); O. Mandel, M. Greiner, A. Widera, T. Rom, T. W. Hänsch, and I. Bloch, Nature (London) **425**, 937 (2003); A. Micheli, D. Jaksch, J. I. Cirac, and P. Zoller, Phys. Rev. A **67**, 013607 (2003).

[2] E. M. Wright, D. F. Walls, and J. C. Garrison, Phys. Rev. Lett. **77**, 2158 (1996); J. Javanainen and M. Wilkens, *ibid.* **78**, 4675 (1997) [see also the comment by A. Leggett, and F. Sols, *ibid.* **81**, 1344 (1998),and the related answer by J. Javanainen and M. Wilkens, *ibid.* **81**, 1345 (1998)]; M. Lewenstein and Li You, *ibid.* **77**, 3489 (1996); Y. Castin and J. Dalibard, Phys. Rev. A **55**, 4330 (1997); P. Villain, M. Lewenstein, R. Dum, Y. Castin, Li You, A. Imamoglu, and T. A. B. Kennedy, J. Mod. Opt. **44**, 1775 (1997); A. Sinatra and Y. Castin, Eur. Phys. J. D **4**, 247 (1998); **8**, 319 (2000).

[3] M. R. Andrews, C. G. Townsend, H. J. Miesner, D. S. Durfee, D. M. Kurn, and W. Ketterle, Science **275**, 637 (1997).

[4] D. S. Hall, M. R. Matthews, C. E. Wieman, and E. A. Cornell, Phys. Rev. Lett. **81**, 1543 (1998).

[5] C. Orzel, A. K. Tuchman, M. L. Fenselau, M. Yasuda, and M. Kasevich, Science **291**, 2386 (2001); M. Greiner, O. Mandel, T. W. Hänsch, and I. Bloch, Nature (London) **419**, 51 (2002); Y. Shin, M. Saba, T. A. Pasquini, W. Ketterle, D. E. Pritchard, and A. E. Leanhardt, Phys. Rev. Lett. **92**, 050405 (2004).

[6] G.-B. Jo, Y. Shin, S. Will, T. A. Pasquini, M. Saba, W. Ketterle, D. E. Pritchard, M. Vengalattore, and M. Prentiss, Phys. Rev. Lett. **98**, 030407 (2007); G.-B. Jo, J.-H. Choi, C. A. Christensen, Y.-R. Lee, T. A. Pasquini, W. Ketterle, and D. E. Pritchard, *ibid.* **99**, 240406 (2007).

[7] A. Widera, S. Trotzky, P. Cheinet, S. Fölling, F. Gerbier, I. Bloch, V. Gritsev, M. D. Lukin, and E. Demler, Phys. Rev. Lett. **100**, 140401 (2008).

[8] S. Hofferberth, I. Lesanovsky, B. Ficher, T. Shumm, and J. Schmiedmayer, Nature (London) **449**, 324 (2007).

[9] A. A. Burkov, M. D. Lukin, and E. Demler, Phys. Rev. Lett. **98**, 200404 (2007).

[10] L. Pitaevskii and S. Stringari, Phys. Rev. Lett. **87**, 180402 (2001).

[11] R. Gati, B. Hemmerling, J. Fölling, M. Albiez, and M. K. Oberthaler, Phys. Rev. Lett. **96**, 130404 (2006).

[12] F. Sols, Physica B **194**, 1389 (1994).

[13] A. Sinatra, Y. Castin, and E. Witkowska, Phys. Rev. A **75**, 033616 (2007).

[14] A. B. Kuklov and J. L. Birman, Phys. Rev. A **63**, 013609 (2000).

[15] D. Jaksch, C. W. Gardiner, K. M. Gheri, and P. Zoller, Phys. Rev. A **58**, 1450 (1998).

[16] R. Graham, Phys. Rev. Lett. **81**, 5262 (1998).

[17] R. Graham, Phys. Rev. A **62**, 023609 (2000).

[18] R. Graham, J. Mod. Opt. **47**, 2615 (2000).

[19] Yu. Kagan, B. V. Svistunov, and G. V. Shlyapnikov, Sov. Phys. JETP **75**, 387 (1992); Yu. Kagan and B. V. Svistunov, Phys. Rev. Lett. **79**, 3331 (1997).

[20] K. Damle, S. N. Majumdar, and S. Sachdev, Phys. Rev. A **54**, 5037 (1996).

[21] K. Góral, M. Gajda, and K. Rzążewski, Opt. Express **8**, 92

(2001); D. Kadio, M. Gajda, and K. Rzążewski, Phys. Rev. A **72**, 013607 (2005).
[22] M. J. Davis, S. A. Morgan, and K. Burnett, Phys. Rev. Lett. **87**, 160402 (2001).
[23] The model Hamiltonian that we consider, being discretized on a lattice, is similar to a Bose-Hubbard model and includes Umklapp processes that do not exist in a real free space gas. There are ways of producing classical field models that are free from this feature, also known as the *aliasing* problem [24,25]. We do not use them here, but we investigate in Appendix B the impact of Umklapp processes on the rates of the Beliaev-Landau damping mechanism, a mechanism that plays a central role in our problem. We find that for modes of energy of order k_BT, Umklapp processes do affect the classical field damping rates calculated on our numerical grid. However, we also find that the naive suppression of these processes by a projection on the same numerical grid strongly underestimates the damping rate of the high energy modes as compared to the exact quantum result, so that for our specific grid choice, keeping the Umklapp processes is actually preferable.
[24] A. A. Norrie, R. J. Ballagh, and C. W. Gardiner, Phys. Rev. A **73**, 043617 (2006).
[25] P. B. Blakie, Phys. Rev. E **78**, 026704 (2008).
[26] Δ stands here for the operator acting on functions on the lattice, such that its eigenvectors are the plane waves $e^{i\mathbf{k}\cdot\mathbf{r}}$ with eigenvalues $-k^2$.
[27] We calculate Var $\varphi(t)$ and its error bars for 5000 time points. These 5000 time points are collected into 100 packets of 50 consecutive points, the ith packet corresponding to a time interval $[t_i, t_i+\Delta t]$. Δt is chosen of the order of the typical correlation time of the condensate phase derivative (see Fig. 3). A temporal average of Var φ over each time interval is then calculated and reported in the figure as a single point at $t_i + \Delta t/2$ with its mean square (time averaged) error bar.
[28] As explained in [13], in Eq. (16) we assume a small noncondensed fraction and we neglect an oscillatory part. We checked analytically, within the Bogoliubov approach and for an infinite cutoff, that the contribution of the oscillatory part of $\dot{\varphi}$ to the correlation function $C(t)$ is a rapidly decreasing function over the time scale $\hbar/\rho g$.
[29] In our classical field model, the field amplitudes on the Bogoliubov modes are given by $b_{\mathbf{k}}(t) = dV\Sigma_{\mathbf{r}} \tilde{U}_k \frac{e^{-i\mathbf{k}\cdot\mathbf{r}}}{\sqrt{V}} e^{-i\theta(t)} \psi_\perp(\mathbf{r},t) - \tilde{V}_k \frac{e^{i\mathbf{k}\cdot\mathbf{r}}}{\sqrt{V}} e^{i\theta(t)} \psi_\perp^*(\mathbf{r},t)$, where $\psi_\perp$ is the component of the field ψ orthogonal to the condensate mode and the real amplitudes $\tilde{U}_k$, $\tilde{V}_k$, normalized as $\tilde{U}_k^2 - \tilde{V}_k^2 = 1$, are given by the usual Bogoliubov theory, here with the modified dispersion relation $\tilde{U}_k + \tilde{V}_k = [\tilde{E}_k/(\tilde{E}_k + 2\rho g)]^{1/4}$.
[30] Y. Castin and R. Dum, Phys. Rev. A **57**, 3008 (1998).
[31] Taking this limit in its true mathematical sense, we eventually reach a discrete regime where the Bogoliubov eigenstates do not form a quasicontinuum, since the energy spacings between the Bogoliubov energy levels are fixed in the Bogoliubov limit whereas the coupling amplitudes among them vanish in this limit. The concept of Beliaev-Landau damping rates may be not appropriate in this discrete regime. To be more rigorous mathematically one should first take the thermodynamic limit and then take the Bogoliubov limit (now formulated as $\rho \to +\infty$ for a fixed ρg). Here we have kept the opposite order for pedagogical reasons, the intuitive reasoning in the Bogoliubov limit allowing one to infer the proportionality of D with $1/N$.
[32] W. V. Liu, Phys. Rev. Lett. **79**, 4056 (1997).
[33] L. P. Pitaevskii and S. Stringari, Phys. Lett. A **235**, 398 (1997).
[34] S. Giorgini, Phys. Rev. A **57**, 2949 (1998).
[35] P. O. Fedichev and G. V. Shlyapnikov, Phys. Rev. A **58**, 3146 (1998).
[36] A. Sinatra, P. O. Fedichev, Y. Castin, J. Dalibard, and G. V. Shlyapnikov, Phys. Rev. Lett. **82**, 251 (1999).
[37] H. Schmidt, K. Góral, F. Floegel, M. Gajda, and K. Rzążewski, J. Opt. B: Quantum Semiclassical Opt. **5**, S96 (2003).
[38] M. Brewczyk, P. Borowski, M. Gajda, and K. Rzążewski, J. Phys. B **37**, 2725 (2004).
[39] C. Lobo, A. Sinatra, and Y. Castin, Phys. Rev. Lett. **92**, 020403 (2004); N. G. Parker and C. S. Adams, *ibid.* **95**, 145301 (2005).
[40] A. A. Norrie, R. J. Ballagh, and C. W. Gardiner, Phys. Rev. Lett. **94**, 040401 (2005).
[41] S. Aubert and C. S. Lam, J. Math. Phys. **44**, 6112 (2003).
[42] A. Sinatra, C. Lobo, and Y. Castin, J. Phys. B **35**, 3599 (2002).
[43] One may note that our approximation for $Q(t)$ is a symmetric matrix, which is not necessarily true for the exact Q at $t > 0$.
[44] C. Mora and Y. Castin, Phys. Rev. A **67**, 053615 (2003).